Transport properties and anisotropy of $Rb_{1-x}Fe_{2-y}Se_2$ single crystals

Chun-Hong Li,[1] Bing Shen,[1] Fei Han,[1] Xiyu Zhu,[1] and Hai-Hu Wen[1,2,*]

[1]*National Laboratory for Superconductivity, Institute of Physics and Beijing National Laboratory for Condensed Matter Physics, Chinese Academy of Sciences, P.O.Box 603, Beijing 100190, China*

[2]*National Laboratory of Solid State Microstructures and Department of Physics, Nanjing University, Nanjing 210093, China*

(Received 30 December 2010; revised manuscript received 21 March 2011; published 26 May 2011)

Single crystals of $Rb_{1-x}Fe_{2-y}Se_2$ are successfully synthesized with superconducting transition temperatures $T_c \approx 31 - 32.5$ K. A clear humplike anomaly of resistivity was observed in the normal state in the temperature region T_{an} of 150 K–186 K, as found in a similar system, $K_xFe_{2-y}Se_2$. It is found that the Meissner screening volume and the superconducting transition temperatures are higher for the sample with higher T_{an}, indicating that the hump of resistivity is strongly related to the superconductivity. The upper critical field has been determined with the magnetic field along the *ab* plane and *c* axis for two typical samples with different T_{an}, yielding an anisotropy of $\Gamma \approx 3.5$ when $T_{an} = 150$ K, while $\Gamma \approx 4.8$ when $T_{an} = 186$ K. The angle-dependent resistivity measured below T_c allow a perfect scaling feature based on the anisotropic Ginzburg–Landau theory, leading to consistent values of the anisotropy. Comparing with the anisotropy determined for $Ba_{0.6}K_{0.4}Fe_2As_2$ and $Ba(Fe_{0.92}Co_{0.08})_2As_2$ using the same method, we find that the present sample is more anisotropic and the Fermi surfaces with stronger two-dimensional characters are expected.

DOI: 10.1103/PhysRevB.83.184521 PACS number(s): 74.25.fc, 74.70.Xa, 74.62.Bf

I. INTRODUCTION

Iron pnictide superconductors have received tremendous attention in past two years since Kamihara *et al.* reported superconductivity at 26 K in $LaFeAsO_{1-x}F_x$.[1] The family of the FeAs-based superconductors has been expanded rapidly. A typical example is the (Ba,Sr)Fe_2As_2 (denoted as FeAs-122) system: The antiferromagnetic order is suppressed, and superconductivity is induced by either K doping in the Ba or Sr sites[2–4] or Co and Ni doping in the Fe sites.[5,6] On the other hand, superconductivity was also found in the FeAs-based parent phase LiFeAs (denoted as FeAs-111)[7–9] and Sr_2VO_3FeAs (denoted as FeAs-21311).[10] Compared with these iron pnictides, FeSe has a more simple structure of only FeSe layers and no toxic arsenic,[11] which shows superconductivity at 8 K at ambient pressure and the transition temperature can be increased dramatically to 37 K under high pressure.[12] Moreover, a recent report showed that superconducting and magnetic properties of $Fe_ySe_xTe_{1-x}$ not only depend on the concentration ratio of Se/Te, but also strongly depend on the interstitial Fe content.[13] Additionally, angle-resolved photoemission spectroscopy(ARPES) showed that the normal state of $FeSe_{0.42}Te_{0.58}$ is a strongly correlated metal, which is significantly different from the FeAs-1111 and FeAs-122 systems.[14] Therefore, the FeSe-layered materials deserve intensive studies for both fundamental physics and potential applications.

Very recently, superconductivity at around 30 K was reported in $K_xFe_2Se_2$ (denoted as FeSe-122),[15] where the potassium ions could be intercalated between the Fe_2Se_2 layers. This discovery was quickly repeated by other groups with the nominal composition $K_{0.8}Fe_2Se_2$.[16] Introducing potassium into the system makes the structure change from 11-type(P4/nmm) to 122-type(I4/mmm). Up to now, system FeSe-122 has given the highest T_c among the FeSe-layered compounds under ambient pressure. Shortly after that, Krzton-Maziopa *et al.* reported the crystal growth of an analog compound $Cs_{0.8}(FeSe_{0.98})_2$.[17] Furthermore, Fang *et al.*[18] synthesized the systematically doped (Tl,K)$Fe_{2-x}Se_2$ and found that the superconductivity might be in proximity to a Mott insulator. If just counting on the electron numbers, one would assume that $A_xFe_2Se_2$ (A = alkaline metals) might be a purely electron doped sample. Thus it is curious to know whether the Fermi surfaces are close to or far different from their relatives Ba(Sr)Fe_2As_2. The anisotropy is one of the important parameters that characterize the electronic properties. In this paper, we report the successful synthesis of the new superconductors $Rb_{1-x}Fe_{2-y}Se_2$. The transition temperatures are estimated to be 31 K–32.5 K. We also present the temperature, magnetic field, and angle dependence of resistivity. Our results point to a higher anisotropy in $Rb_{1-x}Fe_{2-y}Se_2$ compared with electron- and hole-doped Ba(Sr)Fe_2As_2.

II. EXPERIMENT

Single crystals were grown from the melt of the mixture of $Rb_{1-x}Fe_{2-y}Se_2$ using the Bridgeman method. First, $Fe_{2-y}Se_2$ powders were prepared with a high-purity powder of selenium (Alfa Aesar, 99.99%) and iron (Alfa Aesar, 99.9%) by a similar method described in Ref. 19 Then, $Fe_{2-y}Se_2$ and Rb (Alfa Aesar, 99.75%) were mixed in appropriate stoichiometry and were put into alumina crucibles and sealed in an evacuated silica ampoule. The mixture was heated up to 1030 °C and kept over 3 h. Afterward the melt was cooled down to 730 °C with a cooling rate of 6 °C/h, and finally the furnace was cooled to room temperature with the power shut off. Well-formed black crystals were obtained which could be easily cleaved into plates with flat shiny surfaces. However, the fast cooling rate and shorter time at high temperature could cause the mixture to melt nonuniformly and the resulting single crystal to be inhomogeneous. To avoid these defects, we kept the reactants at 1050 °C for 8 h and cooled it down to 700 °C at a rate of 3.5 °C/h. There is a loss of Rb from the melt, and some mixed phases are resulted which consist of

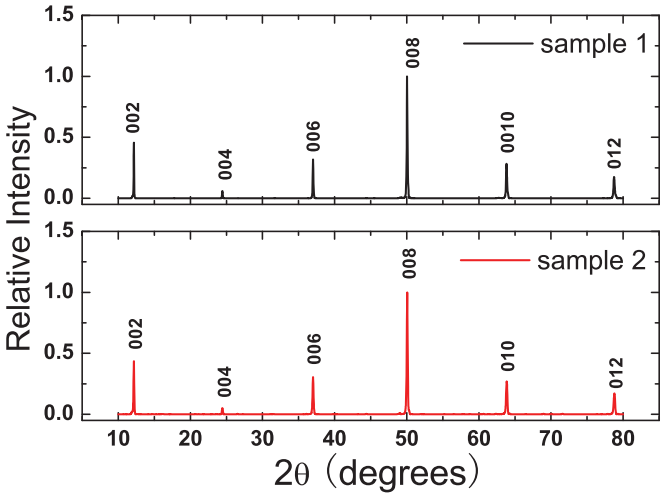

FIG. 1. (Color online) The XRD patterns of $Rb_{1-x}Fe_{2-y}Se_2$ crystals indicate that the $(00l)$ $(l = 2n)$ reflections dominate the pattern.

the desired single crystalline phase and fine polycrystalline material. Therefore the real stoichiometries of $Rb_{1-x}Fe_{2-y}Se_2$ crystals were determined by the inductively coupled plasma (ICP). The crystal structures were characterized by x-ray diffraction (XRD). The dc magnetization measurements were done with a superconducting quantum interference device (SQUID, Quantum Design, MPMS7). The electrical transport data were collected on a Quantum Design instrument, physical property measurement system (PPMS), with magnetic fields up to 9 T. The temperature stabilization was better than 0.1%, and the resolution of the voltmeter was better than 10 nV.

III. RESULTS AND DISCUSSION

Figure 1 shows the XRD patterns of $Rb_{1-x}Fe_{2-y}Se_2$ crystals prepared by different ways. Both samples exhibit good c-axis orientation, as evidenced by the sharp $(00l)$ peaks. The ICP data show that the real stoichiometries of the single crystals are Rb : Fe : Se = 0.76 : 1.62 : 2.00 for sample 1 grown with a fast cooling rate and Rb : Fe : Se = 0.8 : 1.68 : 2.00 for sample 2 grown with slower cooling rate.

The temperature dependence of resistivity for both single crystals of $Rb_{1-x}Fe_{2-y}Se_2$ are presented in Fig. 2(a). A superconducting transition appears at the temperature of 31 K (onset), and the zero resistance appears at 28 K for sample 1 which is similar to that of $K_{0.8}Fe_2Se_2$.[15] The normal state resistivity exhibits a possible semiconductor-to-metal-like transition at around 150 K. Similar behavior was also observed in $K_{0.8}Fe_2Se_2$, although in a different temperature region (about 110 K in $K_{0.8}Fe_2Se_2$),[15] which could also be caused by a structure or magnetic phase transitions. The bulk superconductivity of our sample is also confirmed by dc magnetization measurement which is shown in Fig. 2(b); diamagnetism is clearly observed in both zero-field-cooling and field-cooling measurement. The relatively broad magnetic and resistive transitions of sample 1 may suggest that the sample is still inhomogeneous in composition or the Fe vacancy disorders. It should also be noticed that the

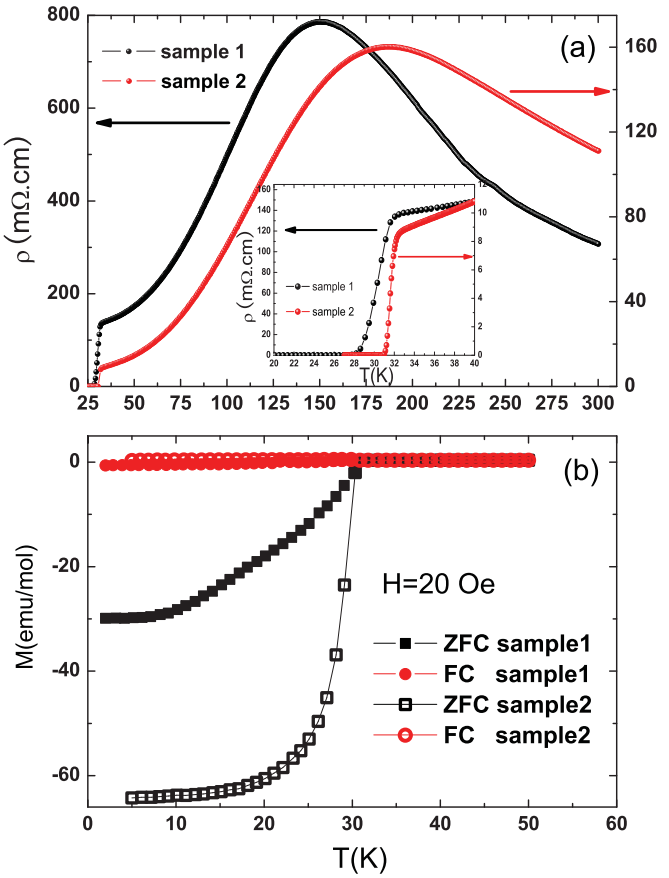

FIG. 2. (Color online) (a) Temperature dependence of resistivity for the $Rb_{1-x}Fe_{2-y}Se_2$ crystal at zero field up to 300 K. A hump of resistivity in the normal state at around 150 K for sample 1 and 186 K for sample 2 can be clearly seen. (b) Temperature dependence of dc magnetization for both zero-field-cooling and field-cooling processes at a magnetic field of $H = 20$ Oe.

absolute value of normal state resistivity is quite large and varies from sample to sample. The maximum value exceeds 700 mΩ cm, which is hundreds of times larger than that in other typical iron-based superconductors. For sample 2 a higher transition temperature of 32.5 K (onset) was observed and zero resistance appeared at 31.5 K. The semiconductor-to-metal-like transition hump in normal state shifts to 186 K. The better diamagnetism and the larger Meissner screening volume were observed in dc magnetization measurements. The higher residual resistivity ratio (R300K/R32.5 K ≈ 14) at 32.5 K and lower normal state resistivity with sharper superconducting transition may indicate less impurities and better homogeneity for sample 2. A rough estimate on the Meissner screening volume by assuming an uniform superconducting condensate at 2 K is about 42% and around 80% for sample 1 and sample 2, respectively. As we know, this kind of estimate is not precise and suffers a modification by counting the demagnetization factor.

In the angle-resolved resistivity measurement, the sample is rotated in the magnetic field where θ is the angle enclosed between the external magnetic field and c axis ($\theta = 0°$ corresponding to the configuration of H // c axis and $\theta = 90°$ to H//ab plane). The current was applied in the ab plane

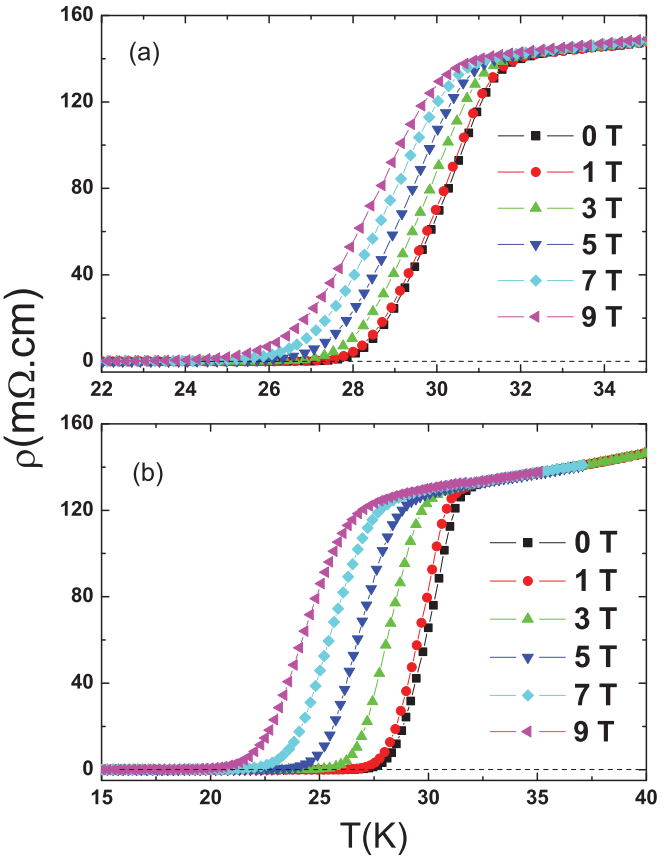

FIG. 3. (Color online) The temperature dependence of resistivity for the $Rb_{0.76}Fe_{1.62}Se_2$ single crystal (sample 1) at zero field and under magnetic fields of (a) $H//ab$ and(b)$H//c$ up to 9 T with increments of 2 T.

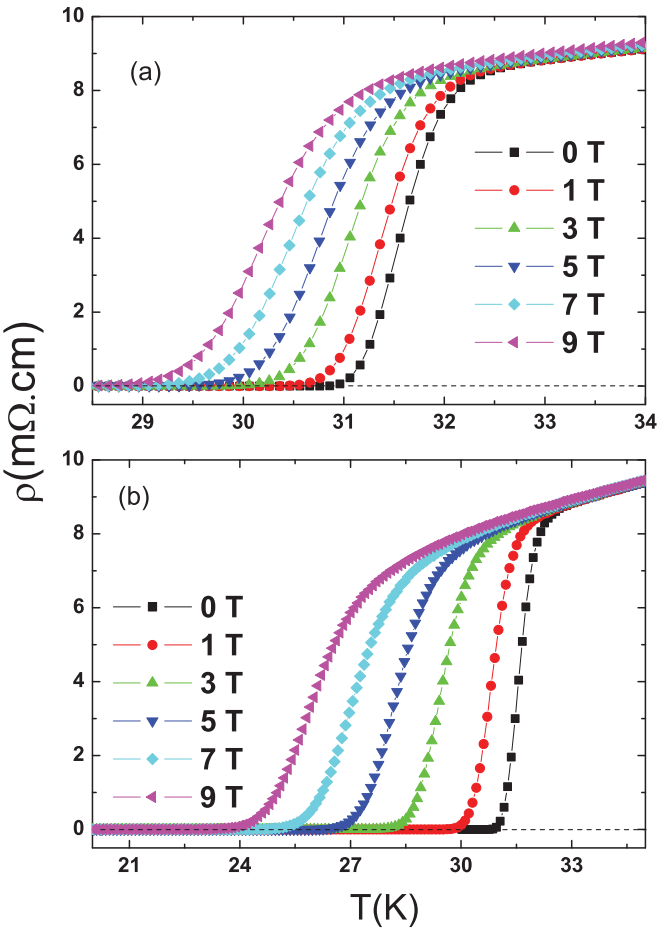

FIG. 4. (Color online) The temperature dependence of resistivity for the $Rb_{0.8}Fe_{1.68}Se_2$ single crystal (sample 2) at zero field and under magnetic fields of (a) $H//ab$ and (b) $H//c$ up to 9 T with increments of 2 T.

and perpendicular to the magnetic field in all cases. The temperature dependence of resistivity from 15 K to 40 K with different magnetic fields applied along the ab plane or c axis for two samples are shown in Figs. 3 and 4. Superconducting transition broadens and is suppressed to the low temperature when applying the magnetic field both parallel to the c axis and within the ab plane. We adopt a criterion of $90\%\rho_n(T)$ to determine the upper critical fields. The upper critical fields of $Rb_{1-x}Fe_{2-y}Se_2$ crystals are determined in this way and shown in Fig. 5. The upper critical fields H_{c2} exhibit a rather linear temperature dependence for both samples and both orientations. Thus we can easily get the values of the slope for two different directions of applying fields. For sample 1 we get $-dH_{c2}^{ab}/dT|_{T_c} = 6.78$ T/K, $-dH_{c2}^{c}/dT|_{T_c} = 1.98$ T/K. For sample 2 we have $-dH_{c2}^{ab}/dT|_{T_c} = 8.84$ T/K, $-dH_{c2}^{c}/dT|_{T_c} = 1.92$ T/K. The value of the slope of two samples for the applying magnetic field within the ab plane significantly exceeds the Pauli limit 1.84 T/K, which may manifest an unconventional mechanism of superconductivity in this material. Using the Werthamer–Helfand–Hohenberg formula $H_{c2}(0) = -0.69\times dH_{c2}/dT|_{T_c}T_c$ (Ref. 20) and taking $T_c = 31$ K and 32.5 K, we can estimate the values of upper critical fields close to zero temperature limit: $H_{c2}^{ab}(0) = 145$ T and $H_{c2}^{c}(0) = 42$ T for sample 1, $H_{c2}^{ab}(0) = 198$ T and $H_{c2}^{c}(0) = 41$ T for sample 2. In determining the $H_{c2}(T)$ near T_c, we used only a relatively low magnetic field; in this case the Zeeman energy is still quite low, and the upper critical field $H_{c2}(T)$ which determines the pair-breaking energy is actually determined by the orbital momentum. Therefore the method we used (the anisotropy derived by the ratio of the upper critical field to the magnetic field along different directions) should be applicable. On the other hand, in the low-temperature region, the upper critical field is very high, and the magnetic interaction will become much stronger compared with the momentum energy; therefore the Pauli limit governs the behavior of $H_{c2}(T)$. According to the Lawrence–Doniach model,[21] the relation between the anisotropy Γ and the upper critical field is given by

$$\Gamma = (m_c/m_{ab})^{1/2} = \xi_{ab}/\xi_c = H_{c2}^{ab}/H_{c2}^{c}, \qquad (1)$$

where H_{c2}^{ab} and H_{c2}^{c} are the upper critical fields with $H \parallel ab$ plane and $H \parallel c$ axis, m_c and m_{ab} are the effective masses when the electrons move along the c axis and ab plane, and ξ_{ab} and ξ_c are coherence length in the ab plane and along the c axis, respectively. From the above data, we can get the anisotropy of the upper critical fields of $Rb_{0.76}Fe_{1.62}Se_2$, $\Gamma \approx 3.5$ and $Rb_{0.8}Fe_{1.68}Se_2$, $\Gamma \approx 4.8$. As a result of faster cooling and a shorter time at a high temperature for sample 1, more impurities and defects may form which are distributed randomly and

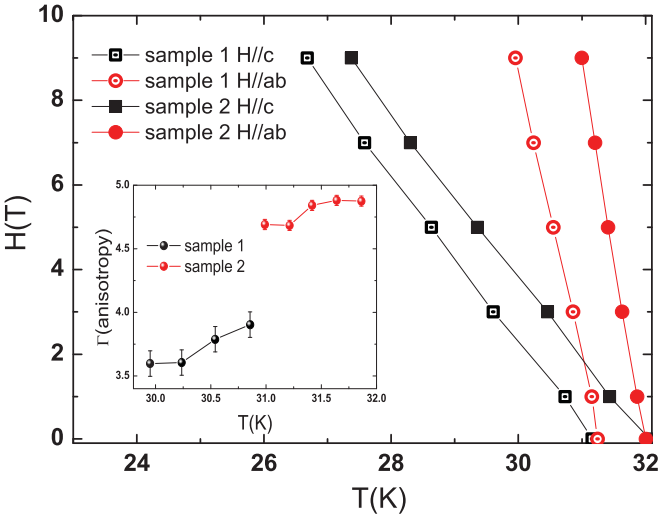

FIG. 5. (Color online) The upper critical fields with the magnetic field parallel to the c axis and within the ab plane for the two $Rb_{1-x}Fe_{2-y}Se_2$ single crystals.

scatter electrons isotropically. The anisotropy of sample 1 is lower than that of sample 2 which may be due to the impurities and defects mashing some instinct anisotropy in these kind of materials. The anisotropy value 4.8 is higher than that in $K_{0.8}Fe_2Se_2$ ($\Gamma \approx 3.6$)[16] and all are quite small compared with high-T_c cuprates, which indicates an encouraging application perspective.

Considering the uncertainties in determining the upper critical field in different formulas and by different criteria, the anisotropy ratio may subject to a modification. One major concern was that the zero-temperature value $H_{c2}(0)$ was determined by using the experimental data near T_c; this concern can be removed by the measurements of angular-dependent resistivity. According to the anisotropic Ginzburg–Landau theory, the effective upper critical field $H_{c2}^{GL}(\theta)$ at an angle θ is given by

$$H_{c2}^{GL}(\theta) = H_{c2}^{ab} \Big/ \sqrt{\sin^2(\theta) + \Gamma^2 \cos^2(\theta)}. \qquad (2)$$

The resistivity at different magnetic fields but a fixed temperature can be scaled with the variable $H/H_{c2}^{GL}(\theta)$. Thus by adjusting Γ, the proper scaling variable $\tilde{H} = H\sqrt{\sin^2(\theta) + \Gamma^2 \cos^2(\theta)}$ is acquired, and then the resistivity measured at different magnetic fields should collapse onto one curve.[22] Figure 6 presents the data of angular dependence of resistivity at 27 K, 28 K for sample 1. At some temperatures, a very small peak centered around $\theta = 90^\circ$ is observed. Normally the resistivity is the lowest when $H \parallel ab$ plane. The little peak appeared at $\theta = 90^\circ$ could be induced by the weak flux pinning channel along the ab plane. This may suggest that there is inhomogeneity along the c axis, which makes the flux easy to move when the field is exactly aligned parallel to ab planes. The curves measured at different magnetic fields but at a fixed temperature are scaled nicely by adjusting Γ. In this treatment only one fitting parameter Γ is employed in the scaling for each temperature, so the value of Γ is more reliable than the one determined from the ratio of H_{c2}^{ab} and H_{c2}^{c}, which may be affected by using different criterion. At 27 K and 28 K the anisotropies Γ are found to be 2.9 ± 0.2 and

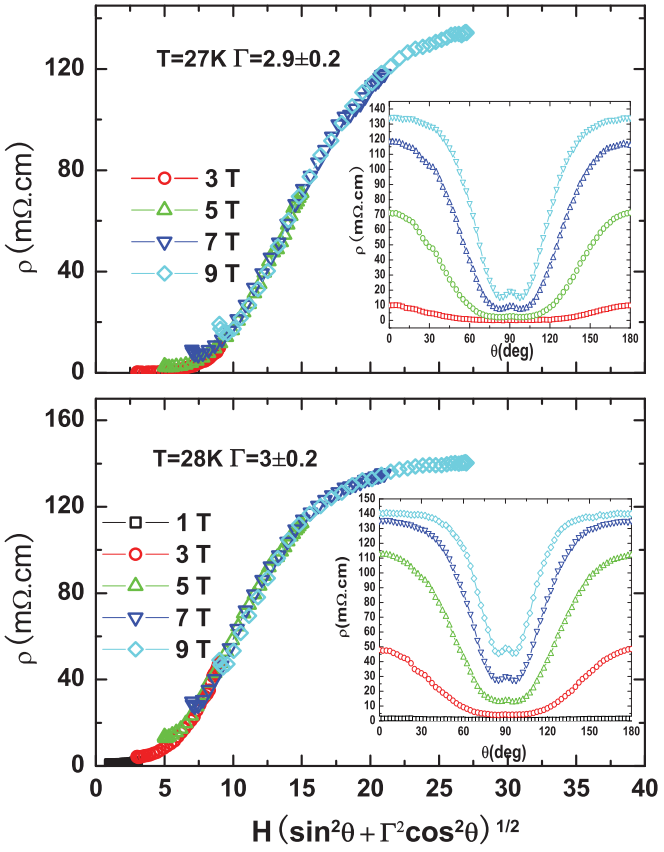

FIG. 6. (Color online) Scaling of the resistivity versus $\tilde{H} = H\sqrt{\sin^2(\theta) + \Gamma^2 \cos^2(\theta)}$ at 27 K, 28 K in different magnetic fields for sample 1. The curves are measured at the same temperature but different magnetic fields are scaled nicely by adjusting the value of Γ. The inset presents the angular dependence of resistance for the $Rb_{0.76}Fe_{1.62}Se_2$ single crystal (sample 1).

3 ± 0.2, respectively. The results agree very well with the value determined by the ratio of H_{c2}^{ab} and H_{c2}^{c}, which implies the validity of the values determined in this work. It is interesting to mention that the anisotropy determined using the ratio of H_{c2}^{ab} and H_{c2}^{c} is quite close to that determined using the normal state resistivity ρ_c/ρ_{ab} at around T_c by Hu *et al.*[23] Though an abnormal cusp at 90° can be observed in the inset of Fig. 6 which suggests some impurities or defect scattering, the sufficient data at other angles can also give a good scaling curves at different magnetic fields. In the same way, the Γ obtained at 29 K and 30 K are 3.3 ± 0.1 and 3.6 ± 0.1, which are a little larger than those at 27 K and 28 K. The anisotropy produced by the anisotropic Ginzburg–Landau theory is agreeable with that produced by the ratio of upper critical field. The data of angular dependence of resistivity at 29 K, 30 K for sample 2 are presented in Fig. 7. No abnormal cusp-shaped feature centered around $\theta = 90^\circ$ like sample 1 is observed, and the data at different magnetic fields can nicely scale onto one curve. In the same method the anisotropy of sample 2 at 27 K, 28 K, 29 K, 30 K, and 31 K are derived to be 3.5 ± 0.1, 4.1 ± 0.08, 4.4 ± 0.04, 4.85 ± 0.04, and 5 ± 0.02 respectively. The Γ is agreeable with the former value determined by the ratio of upper critical field and higher than that of sample 1. Due

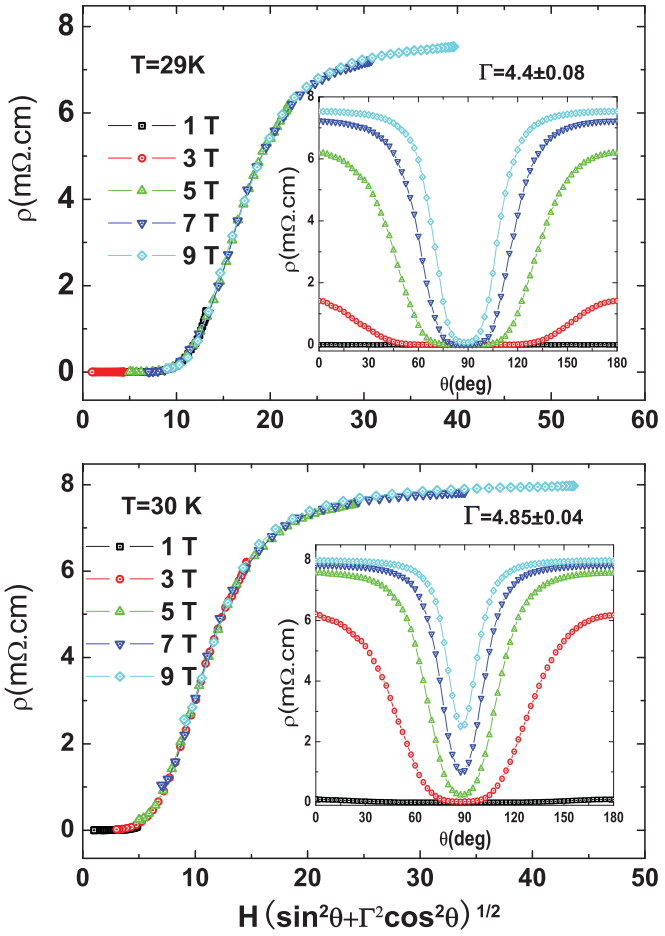

FIG. 7. (Color online) Scaling of the resistivity versus $\tilde{H} = H\sqrt{\sin^2(\theta) + \Gamma^2\cos^2(\theta)}$ at 29 K, 30 K in different magnetic fields for sample 2. The curves are measured at the same temperature, but different magnetic fields are scaled nicely by adjusting the value of Γ. The inset presents the angular dependence of resistance for the $Rb_{0.8}Fe_{1.68}Se_2$ single crystal (sample 2).

to the slow cooling and longer time at high temperatures in the growth process, there are less impurities and defects with lower resistivity in the normal state and a higher residual resistivity ratio (R300K/R32K ≈ 14) in sample 2. Correspondingly, the semiconductor-to-metal-like transition hump in normal state shifts to 186 K, which coincides with the large Meissner screening volume and the sharper superconductivity transition. Compared with the anisotropy in other FeAs-based superconductors, the value of anisotropy is similar to 5 in $NdFeAsO_{1-x}F_x$ and higher than 2–2.5 in $Ba_{1-x}K_xFe_2As_2$.

The anisotropy determined by the anisotropic Ginzburg–Landau theory at different temperatures of $Rb_{0.76}Fe_{1.62}Se_2$, $Rb_{0.80}Fe_{1.68}Se_2$, $Ba_{0.6}K_{0.4}Fe_2As_2$, and $Ba(Fe_{0.92}Co_{0.08})_2As_2$ single crystals are shown in Fig. 8. It is found that the anisotropy of $Rb_{1-x}Fe_{2-y}Se_2$ decreases slightly with decreasing temperature. This kind of temperature dependence of $\Gamma(T)$ is consistent with other FeAs-122 superconductors, such as $Ba_{0.6}K_{0.4}Fe_2As_2$, $Ba(Fe_{0.92}Co_{0.08})_2As_2$, etc. This may be understood as the multiband effect or the effect due to the gradual setting in of pair breaking by the spin-paramagnetic

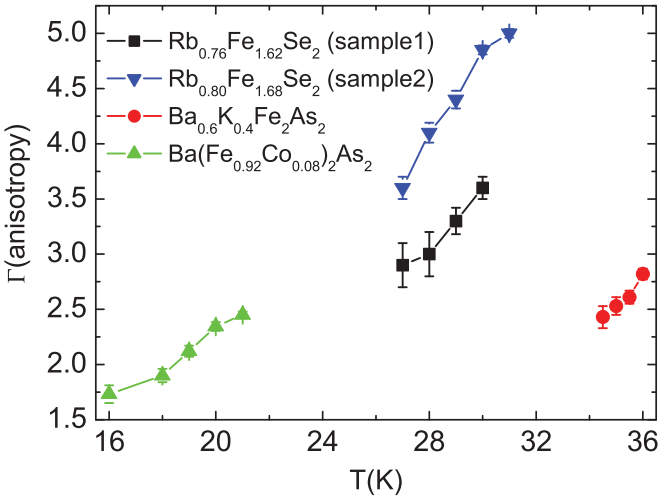

FIG. 8. (Color online) The comparison of anisotropy for the $Rb_{0.76}Fe_{1.62}Se_2$, $Rb_{0.8}Fe_{1.68}Se_2$, $Ba_{0.6}K_{0.4}Fe_2As_2$, and $Ba(Fe_{0.92}Co_{0.08})_2As_2$ single crystals.

effect which requires $H_{c2}^{ab} = H_{c2}^{c}$ in the low-temperature and high-field limit. It should be noted that the good scaling behavior suggests a field-independent anisotropy in the temperature and field range we investigated.[24] The anisotropy of $Rb_{1-x}Fe_{2-y}Se_2$ is similar to that of the FeAs-1111 family, such as $NdFeAsO_{1-x}F_x$, while it is higher than that in hole- and electron-doped FeAs-122 superconductors and KFe_2As_2 with the same structure.[25] It is, however, very strange that KFe_2As_2 and $K_xFe_2Se_2$, should reside in the two terminals of the phase diagram; The former is strongly hole doped, while the latter is heavily electron doped. The larger anisotropy in $K_xFe_2Se_2$ may suggest a more two-dimensional Fermi surface in this material. The difference between the anisotropy in $Ba_{0.6}K_{0.4}Fe_2As_2$ and $Rb_{1-x}Fe_{2-y}Se_2$ may hinge on that the latter has a less warped Fermi surface. Meanwhile, the higher superconducting transition temperature with the better diamagnetism and the sharper superconducting transition is accompanied by the higher T_{an} which indicates the hump of resistivity is closely related to the superconductivity. Our results here should be stimulating in fulfilling a quantitative calculation and further studying on the electronic structure of this new family, and ultimately providing an understanding to the underlying mechanism of superconductivity.

IV. CONCLUSION

In conclusion, we successfully fabricated single crystals of $Rb_{1-x}Fe_{2-y}Se_2$ with the superconducting transition temperatures $T_c \approx 31 - 32.5$ K. A clear anomaly of the resistivity was observed in the normal state at about 150–186 K. We also determined the upper critical fields along the *ab* plane and *c* axis for two typical samples with different T_{an}, which yield an anisotropy of $\Gamma \approx 3.5$ when $T_{an} = 150$ K, while $\Gamma \approx 4.8$ when $T_{an} = 186$ K. It is found that the Meissner screening volume and the superconducting transition temperatures are higher for the sample with higher T_{an}. The angle-dependent resistivity measured below T_c allows a perfect scaling based on the anisotropic Ginzburg–Landau theory. The consistent value

of the anisotropy is acquired which decreases from about 3.6 at 30 K around T_c to 2.9 at 27 K for sample 1 and from about 5 at 31 K around T_c to 3.5 at 27 K. Comparing with the anisotropy determined for $Ba_{0.6}K_{0.4}Fe_2As_2$ and $Ba(Fe_{0.92}Co_{0.08})_2As_2$ using the same method, we expect that the Fermi surfaces in the new system $A_xFe_2Se_2$ are less warped.

ACKNOWLEDGMENTS

This work is supported by the Ministry of Science and Technology of China (973 project No: 2011CBA00102), the Natural Science Foundation of China (project number: 51002180), and Chinese Academy of Sciences.

*hhwen@nju.edu.cn

[1] Y. Kamihara, T. Watanabe, M. Hirano, and H. Hosono, J. Am. Chem. Soc. **130**, 3296 (2008).

[2] M. Rotter, M. Tegel, and D. Johrendt, Phys. Rev. Lett. **101**, 107006 (2008).

[3] N. Ni, S. L. Bud'ko, A. Kreyssig, S. Nandi, G. E. Rustan, A. I. Goldman, S. Gupta, J. D. Corbett, A. Kracher, and P. C. Canfield, Phys. Rev. B **78**, 014507 (2008).

[4] K. Sasmal, B. Lv, B. lorenz, A. M. Guloy, F. Chen, Y. Y. Xue, and C. W. Chu, Phys. Rev. Lett. **101**, 107007 (2008).

[5] A. S. Sefat, R. Jin, M. A. McGuire, B. C. Sales, D. J. Singh, and D. Mandrus, Phys. Rev. Lett. **101**, 117004 (2008).

[6] J. H. Chu, J. G. Analytis, C. Kucharczyk, and I. R. Fisher, Phys. Rev. B **79**, 014506 (2009).

[7] X. C. Wang, Q. Q. Liu, Y. X. Lv, W. B. Gao, L. X. Yang, R. C. Yu, F. Y. Li, and C. Q. Jin, Solid State Commun. **148**, 538 (2008).

[8] J. H. Tapp, Z. Tang, B. Lv, K. Sasmal, B. Lorenz, P. C. W. Chu, and A. M. Guloy, Phys. Rev. B **78**, 060505(R) (2008).

[9] M. J. Pitcher, D. R. Parker, P. Adamson, S. J. C. Herkelrath, A. T. Boothroyd, and S. J. Clarke, Chem. Commun. **45**, 5918-20 (2008).

[10] X. Y. Zhu, F. Han, G. Mu, P. Cheng, B. Shen, B. Zeng, and H. H. Wen, Phys. Rev. B **79**, 220512(R) (2009).

[11] F.-C. Hsu, J.-Y. Luo, K.-W. Yeh, T.-K. Chen, T.-W. Huang, P. M. Wu, Y.-C. Lee, Y.-L. Huang, Y. Y. Chu, D.-C. Yan, and M.-K. Wu, Proc. Natl. Acad. Sci. USA **105**, 14262 (2008).

[12] S. Margadonna, Y. Takabayashi, Y. Ohishi, Y. Mizuguchi, Y. Takano, T. Kagayama, T. Nakagawa, M. Takata, and K. Prassides, Phys. Rev. B **80**, 064506 (2009).

[13] L. Zhang, D. J. Singh, and M. H. Du, Phys. Rev. B **79**, 012506 (2009).

[14] A. Tamai, A. Y. Ganin, E. Rozbicki, J. Bacsa, W. Meevasana, P. D. C. King, M. Caffio, R. Schaub, S. Margadonna, K. Prassides, M. J. Rosseinsky, and F. Baumberger, Phys. Rev. Lett. **104**, 097002 (2010).

[15] J. Guo, S. Jin, G. Wang, S. Wang, K. Zhu, T. Zhou, M. He, and X. Chen, Phys. Rev. B **82**, 180520(R) (2010).

[16] Y. Mizuguchi, H. Takeya, Y. Kawasaki, T. Ozaki, S. Tsuda, T. Yamaguchi, and Y. Takano, e-print arXiv:1012.4950 [cond-mat.supr-con].

[17] A. Krzton-Maziopa, Z. Shermadini, E. Pomjakushina, V. Pomjakushin, M. Bendele, A. Amato, R. Khasanov, H. Luetkens, and K. Conder, e-print arXiv:1012.3637 [cond-mat.supr-con].

[18] M. H. Fang, H. D. Wang, C. H. Dong, Z. J. Li, C. M. Feng, J. Chen, and H. Q. Yuan, e-print arXiv:1012.5236 [cond-mat.supr-con].

[19] F. C. Hsu, J. Y. Luo, K. W. Yeh, T. K. Chen, T. W. Huang, P. M. Wu, Y. C. Lee, Y. L. Huang, Y. Y. Chu, D. C. Yan, and M. K. Wu, Proc. Natl. Acad. Sci. USA **105**, 14262 (2008).

[20] N. R. Werthamer, E. Helfand, and P. C. Hohenberg, Phys. Rev. **147**, 295 (1966).

[21] W. E. Lawrence and S. Doniach, in proceedings of the 12th International Conference on low Temperature Phyics, edited by E. Kanda (Keigaku, Tokyo, 1971), p. 361.

[22] G. Blatter, V. B. Geshkenbein, and A. I. Larkin, Phys. Rev. Lett. **68**, 875 (1992).

[23] R. Hu, K. Cho, H. Kim, H. Hodovanets, W. E. Straszheim, M. A. Tanatar, R. Prozorov, S. L. Budko, and P. C. Canfield, e-print arXiv:1102.1931 [cond-mat.supr-con].

[24] Z. S. Wang, H. Q. Luo, C. Ren, and H. H. Wen, Phys. Rev. B **78**, 140501(R) (2008).

[25] T. Terashima, M. Kimata, H. Satsukawa, A. Harada, K. Hazama, S. Uji, H. Harima, G. F. Chen, J. L. Luo, and N. L. Wang, J. Phys. Soc. Jpn. **78**, 063702 (2009).